PWI and DWI Systems in Modern GDI Engines: Optimization and Comparison Part II: Reacting Flow Analysis

PWI and DWI Systems in Modern GDI Engines: Optimization and Comparison Part II: Reacting Flow Analysis

Falfari, S., Bianchi, G.M.
DIN Department of Industrial Engineering, University of Bologna

Pulga, L., Forte, C.
Nais srl

Abstract

In the current scenario characterized by continuous reduction of the allowed limits of mean engine-out emissions over the test-cycles together with the necessity of limiting the local peaks too, which will lead in the next future to the adoption of stoichiometric mixtures at full load conditions, water injection is one of the exploited technologies. At full power, at stoichiometric conditions, water injection is thought to help contributing towards more efficient engines, because its anti-knock attitude in S.I. engine applications. To perform a rapid optimization of the main parameters involved by the water injection process, it is necessary to have reliable CFD methodologies capable of capturing the most important phenomena: indeed, it must be considered that the injection of water changes both the thermodynamic (due to the temperature reduction) and the chemical behavior of the mixture.

In the present work, a methodology for the CFD simulation of non-reacting flow conditions in GDI engines using AVL Fire code v. 2020 is applied for the assessment of the water injection. The non-reacting flow CFD analysis has been presented in PART I paper by the authors [7]. Both Port Water Injection (PWI) and Direct Water Injection (DWI) have been tested for the same baseline engine configuration and the main results have been checked in terms thermodynamic, fluid-dynamic properties and mixture quality. The water injection solutions, both PWI and DWI, have been run at full power condition, at the same rated power engine speed by varying the injection pressure and timing, the quantity of injected water and the engine baseline configuration (geometric Compression Ratio CR has been varied). Best solutions for both strategies have been analyzed under reacting flow conditions in the present work, which deals with the reacting-flow study only. The ECFM-3Z model adopted for combustion and knock simulations takes advantages by the adoption of correlations for the laminar flame speed, flame thickness and ignition delay times prediction obtained by a detailed chemistry calculation in order to account for the modified chemical behavior of the mixture due to the added water vapor. This improved methodological approach allows considering both the fluid-dynamics aspects (in terms of turbulence level close to ignition time and average in the combustion chamber), the mixture quality and the chemical properties of the mixture (first of all the laminar flame speed) related to the water injection. The main result for the design process is the need of finding the best trade-off between the cooling of the unburnt mixture (reducing the knock risk), the need to preserve the turbulence and the flame laminar speed: the latter is already penalized by the cooling of the charge. Finally, a comparison was made between the DWI and PWI systems in the light of the above.

Introduction

Climate change is one of the most critical issues to be faced by our society in the coming future. CO_2 emissions reductions and development of technologies aimed to increase engine efficiency are the current guidelines for new engine concept design. In 2017 the EU Commission issued a notice on the new policy concerning the fuel enrichment for limiting the Turbine Inlet Temperature (TiT), aimed to protect components such as turbine. This strategy has been found to increase dramatically CO emissions since CO cannot be handled by the Three Ways Catalyst (TWC) under rich combustion conditions. According to the perspective of large CO emissions increase due to fuel enrichment strategy, the development of S.I. engines operating at stoichiometric conditions in the overall map is strongly recommended in the next future. All those AES found to increase emissions might not be authorized in the next future.

Depending on the engine type, the most demanding points of the RDE test cycle are generally those close to full power since the exhaust gas temperature at turbine inlet may increase above the limits because of the lack of fuel cooling effect. In this scenario, the water injection is one of the exploited technologies, because its anti-knock attitude in S.I. engine applications [1-4], together with the use of overexpansion cycle (Miller or Atkinson), cooled EGR, improved turbochargers, ignition system technology, alternative fuels. It must be considered that the injection of water changes both the thermodynamic and the chemical behavior of the mixture [5-6]. If the thermodynamic effects can be currently well captured with standard RANS CFD simulations, the effects of the water dilution on combustion duration, and indirectly also on the TiT and the engine knock limit, ask for the accurate prediction of the flame laminar speed, the flame laminar thickness and the auto-ignition time.

In the present work, a comprehensive methodology for the CFD simulation of reacting cycles is applied for the assessment of high-*bmep*-high *power* SI GDI turbocharged engine under water injection operation. Both Port Water Injection (PWI) and Direct Water Injection (DWI) architectures have been tested for the same baseline engine configuration and the main results have been presented in the PART I paper [7]: starting from the baseline engine, for pursuing the target of improving the engine efficiency over the whole engine map for CO_2 emission reduction and maintaining good performance level, the compression ratio CR of the baseline engine has been increased. Water injection might allow to use higher CR with limited penalties on performance. Best solutions for both injection strategies have been analyzed under reacting flow conditions in the present paper. The ECFM-3Z model adopted for combustion and knock simulations takes advantages by the adoption of correlations for the laminar flame speed, flame

thickness and ignition delay times prediction obtained by a detailed chemistry calculation [2]. The adopted methodology is capable of capturing not only the thermodynamic effects of water injection but also the chemical kinetics aspects related to the mixture water dilution whose prediction is mandatory for addressing the engine design according to different goals: a) complying with new emission directives and limits, b) turbine inlet temperature constraints, c) minimization of the *bsfc*, d) possibly engine power increase.

The research activity presented in this paper has been split in the following main items, corresponding to as many paragraphs:

1. Literature review.
2. Engine specifications.
3. Simulation setup.
4. Water injection system and engine configurations: reacting flow results.

LITERATURE SURVEY

The main positive aspect of the water injection is its strong mixture cooling capability which also increases the engine volumetric efficiency thanks to its high latent heat of vaporization. Nevertheless, besides it, it is well known that the water vapor acts as a mixture diluter, thus diminishing the reactants burning rate and changing the auto-ignition delay time [3-6]. Many authors have studied the effect of the water injection on the combustion efficiency. In [8] the authors have reported a summary of the main benefits of water injection on boosted SI engines. The water acts as a heat sink reducing the mixture temperature during the compression phase: the added water also changes the ratio of specific heats of the charge mixture and slightly dilutes the oxygen concentration. These changes reduce the knock tendency and the NOx emissions. Specific torque output is increased by the engine boosting, while engine downsizing, aimed to maintain a proper brake torque output, causes engine to run with higher brake mean effective pressure (BMEP), as highlighted in [9].

For clarity's sake, here some other scientific works have been cited and subdivided on the base of the main discussed topic. The main topics are:

1. Chemical kinetics evaluation of the actual chemical property of the fresh mixture if water vapor is added.
2. Effect of water injection on the combustion process (cooling effect, slowing down of the flame speed).

CHEMICAL KINETICS ANALYSIS AIMED TO THE DEFINITION OF THE WATER-ADDED-MIXTURE CHEMICAL PROPERTIES: From an engineering point of view, the accurate (not easy) prediction of the thermodynamics and physical effects of liquid and vapor water is not sufficient since the trade-off between combustion duration, knock tendency and TiT asks for complex chemistry. In RANS CFD combustion simulations, a very good and effective mean to deal with this requirement is to use combustion models based on the flamelet approach (i.e. ECFM-3Z, G-Equation models) which account for both the detailed air-fuel chemistry and flame-turbulence interaction assuming that the turbulent flame front can be regarded as an aggregate of smaller laminar flames [10, 11, 12]. The description of the chemical kinetics properties of the mixture is summarized by the unstretched laminar flame speed and thickness. The definition of these quantities has relied for several years on well-established correlations derived from experimental data [13]. The main limitation of this approach is the restricted range of the validation domain, which is usually very far from the conditions reached during the operations of modern engines, and the lack of flexibility with respect to the mixture formulation. To overcome these limitations, in recent years research has relied more heavily on detailed chemical kinetics simulations of laminar flames [14, 15] to populate look-up tables or generate enough data to fit new correlations. Fandakovet et al. [15, 16] presented a detailed reaction kinetics mechanism focused on the prediction of the low- and high-temperature mixture ignition stages (two-stage ignition) and of the temperature increase resulting from the low-temperature ignition.

The authors of the present paper have developed a research activity [2] aimed to define and validate an end to end methodology based on chemical kinetics reduction and machine learning algorithms for the definition of the reaction properties needed for the CFD simulation of internal combustion engines also in the presence of water vapor. This approach relied on the previous ones by Pulga et al. [17, 18]. The correlations deriving from these datasets have been applied to the RANS-CFD combustion simulations presented in this work.

COMBUSTION ANALYSIS UNDER WATER INJECTION STRATEGY: In [18] Pulga et al. reported as the addition of water, which acts as a diluent, is expected to reduce the Laminar Flame Speed (LFS) of the reacting mixture, which is an essential property required to calculate the reaction rate in most combustion models. Berni et al. [19] studied Port Water Injection on a high performance turbocharged GDI engine, highlighting benefits in terms of combustion efficiency increase and related reduction in brake specific fuel consumption. Battistoni et al. [20] and Netzer et al. [21] have worked on the effect of the water on the combustion process. In [22] and [23] the authors studied the potential benefits of the PWI water injection in a PFI turbocharged engine, combining the effect of the water injection with the effect of the exhaust gas recirculation for reducing the exhaust gas temperature. In [23] the focus of the work was to find the same IMEP level and detonation limit of the rich mixture but working with a stoichiometric mixture and compensating the difference in the fuel mass with the corresponding water mass. In [24] the authors studied for a naturally aspirated GDI engine equipped by Direct Water Injector the effects of water injector orientation and spray angle on the reduction of NOx and soot emissions. In [25] the influence of water injection on the combustion process and raw emissions was analyzed experimentally on a single-cylinder research engine with direct and indirect water injection. The authors highlighted that, even though water injection initially slows down the combustion process, both injection concepts allow shifting the knock limit and reducing the exhaust gas temperature. In [26] Vacca et al. aimed to the comprehension of multiple thermodynamic effects related to water injection and to the enhancement of combustion efficiency through 3D-CFD simulations. Measurements have been performed for indirect/direct water injection in the single-cylinder engine to assess water break-up, wall wetting, spray interaction and penetration. The authors have also experimentally tested several injection strategies, varying start of injection, injection pressure, and water to fuel ratio. Last of all, they have considered the effect of ambient air humidity on water injection strategy. In [1] authors have

summarized the main advantages/drawback of both PWI and DWI architectures coming from the literature review. They listed the main limitations of water injection: i) combustion duration increase; ii) combustion efficiency decrease due to increase of HC and CO emissions; iii) a negative impact of the lowering of the polytropic index which limits indicated efficiency improvement; iv) reduced combustion stability which is associated with its lengthening, with IMEP covariances greater than 2%. In [27] Millo et al. combined water injection with CR increase and Miller cycle on a 1.4L 4 cylinders GDI engine, equipped with a PW injector. They have tested two compression ratios: 10:1 and 13:1. The increase of CR is beneficial at low/part load, allowing a fuel consumption reduction of 4.5%. At high load, for mitigating knock occurrence, the water injection strategy was necessary: it helps mitigate the negative impact of higher CR on the maximum power. In [28] Paltrinieri et al. studied water injection applicability at high specific power engine requirements. An experimental campaign, then followed by 3D CFD simulations, on a single cylinder engine has been carried out to highlight port water injection benefits and possible limitations at high engine speed and loads. To decrease the *bsfc* in the whole engine map, water injection has been studied in combination with Miller cycle, which allows to have long expansion stroke while maintaining low effective compression ratio. The over-expanded cycle allows the engine to run with high efficiency in part-load conditions and knock mitigation potential at high engine load and speed. They highlighted that by actuating early IVC there is a premature dissipation of the organized fluid macro-structures inside the cylinder, thus evolving in a steep decay of turbulence level at the combustion onset.

THE ENGINE SPECIFICATIONS

A high-bmep and high-power S.I. GDI turbo-charged engine has been virtually designed at the University of Bologna and slightly modified compared to the previous one [4]. In Figure 1 the engine is visible, in the DWI version in Figure 1a and in the PWI configuration in Figure 1b, respectively, with the same compression ratio for both. It is to note that the two engine configurations, respectively PWI and DWI, are not exactly the same because of the presence of the DWI injector in the DWI engine, below the suction duct. Anyway, the trapped mass has been kept constant on the whole simulation map.

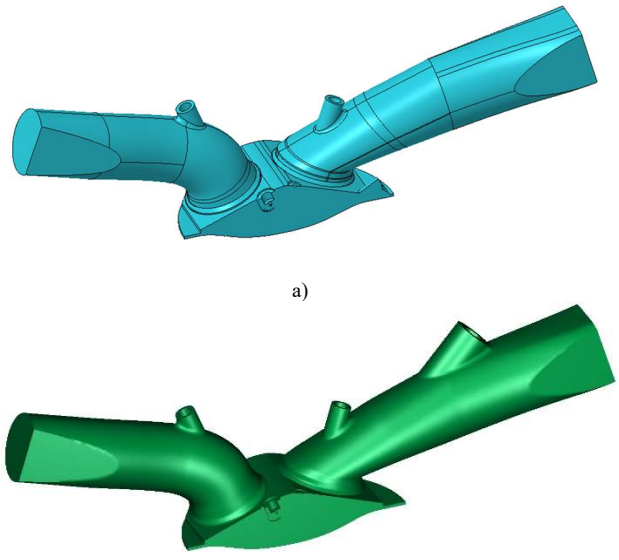

a)

b)

Figure 1. Virtual engine with a) DWI system; b) PWI system

Table 1. Gasoline and water injector characteristics

	GASOLINE	DWI	PWI
Number of holes [-]	8.0	5.0	2.0
Injection pressure [bar]	350.0	50.0/150.0	10.0
Injection temperature [K]	313.0	313.0	313.0
HFR [cm^3/s]	20.0	17.0	17.0
Hole geometric diameter [µm]	188.0	220.0	347.0

Table 2. Main characteristics of the engine

Unit Displacement [cm^3]	471.05
Stroke S [mm]	85.00 / 95.00
Bore D [mm]	84.00
Conrod length [mm]	165.60
Number of valves	4.00
S/D [-]	1.01
Intake D_V/D [-]	0.36
Exhaust D_V/D [-]	0.33
Compression ratios	9.50:1.00 / 10.50:1.00
Squish Height [mm]	1.10

Table 3. Engine operation point at full power

Engine speed [rpm]	7000.0
Engine load	100.0%
Spark Advance	Sweep until knock limited
Mixture index (w/o water) [-]	1.0
Boost pressure [bar]	2.7
Max BMEP [bar]	26.6
Inlet valve opening [CA deg. ATDC]	362.0
Inlet valve closing [CA deg. ATDC]	598.0
Exhaust valve opening [CA deg. ATDC]	136.0
Exhaust valve closing [CA deg. ATDC]	376.0

The water injector spray targeting was carefully chosen in both configurations to minimize the wall impingement, especially on the piston periphery, and therefore to promote the water evaporation within the airstream and from the liquid film formed on walls. The injector in the DWI case is mounted on the intake side of the engine head. This helps in the overall drawing of the engine head and it allows larger free spray path between the injector and the cylinder or piston surfaces. Moreover, the water spray beam orientation was set to promote the interaction between the water plumes and the in-cylinder air-flow field, enhancing the water evaporation rate. The injector characteristics have been resumed in Table 1 [7]. The fuel injector is centrally located with a spray targeted to spark plug for promoting combustion during cat-heating phase. Table 2 resumes the main specifications of the adopted high-bmep engine. The operating point considers the full power condition listed in Table 3.

DESCRIPTION OF THE SIMULATION ENVIRONMENT

The boundary and the initial conditions for the CFD simulations at the considered operating point have been derived by running one-dimensional simulations using the open source code OpenWAM. More details can be found in the PART I paper, concerning non-reacting flow simulations [7].

The engine cycle three-dimensional CFD simulations, whose setup is shown in Table 4, were performed following a multi-cycle approach: the presented results refer to the last converged engine cycle.

Table 4. Main settings for CFD simulations – REACTING FLOW

Start angle	330 CA deg. ATDC
End angle	856 CA deg. ATDC – corresponding to EVO
Turbulence model	K-z-f
Wall heat model	Hybrid wall treatment
Law of the wall	Standard + Han-Reitz
Evaporation model	Spalding
Wallfilm evaporation model	Combined
Wallfilm entrainment model	Schadel - Hanratty
Wallfilm splashing model	Kuhnke
Atomization model	Slightly modified version of the model presented in [29]
Breakup model	
Combustion model	ECFM-3Z adopting correlations for LFS, flame thickness and auto-ignition delay time
Ignition model	Lagrangian ignition model [11, 12]
Knock model	Two steps autoignition model based on [14]

Differencing schemes are second order for mass, momentum, energy, while turbulence is resolved with a second order blended scheme. The solution is converged when the residual error for each equation is below the tolerance threshold of 1e-4. Reacting flow simulations have been performed. Non-reacting flow simulations have been stopped at TDC of the converged cycle and they are aimed to assess the behavior of water injection system and operating conditions. Combustion system half-geometry domain has been considered because of the symmetry conditions. The computational mesh has 506.000 cells at TDC has been set. The parameter s is used to measure the injected water mass per cycle and cylinder, and it is defined as the ratio between the injected water mass and the stoichiometric fuel mass of the given engine operation point.

3D-CFD SIMULATIONS OF INDIRECT/DIRECT WATER INJECTION STRATEGIES

For the future emission regulations, it might be necessary to run gasoline engines under stoichiometric conditions. To limit at full power the exhaust temperature, compensating the lack of the mixture enrichment strategy, in the present work both PWI and DWI architectures have been deeply analyzed and compared the one with the other at stoichiometric conditions. The current turbocharged SI engines overfueling strategy (component protection strategy) adopts a mixture index variable in the range among λ 0.75 and λ 0.85, where the extra fuel is used for cooling down the fresh mixture, for limiting TiT under the threshold value (i.e., 950 °C) imposed by the current turbine material thermal limits. For highlighting the consequences of such a shift from rich mixture to stoichiometric mixture operations, simulations for λ 0.75, λ 0.85 and λ 1.0 have been performed under reacting flow conditions. They fuel-only strategies simulations represent a mandatory reference system for the assessment of the simulation results obtained by applying the water injection strategy under stoichiometric conditions. In the next part of the paper PWI and DWI architectures under reacting flow conditions will be analyzed: these cases represent the best choices or the most interesting ones for each injection system compared with each other and with the fuel-only case at variable mixture index (λ equal to 0.75, 0.85 and 1.0), as shown by non-reacting flow simulations presented in PART I work [7]. They have been reported in Table 5: they are all characterized by the same nominal rated power. In Table 6 the injected masses of fuel and water have been reported for the cases of Table 5. Finally, in Table 7 the SOI/EOI times for each case of Table 5 are visible. For seeking of clarity, only the main results of the non-reacting flow analysis [7] have been reported here:

1. All the cases of Table 5 have at least the 90% of evaporated mass from injected water within TDC under non-reacting flow conditions: this high-demanding constraint has been pursued for limiting the water consumption (refilling frequency) and the presence of liquid water at TDC in the chamber, but it might penalize the whole cooling efficiency which could take advantage by large amount of injected water mass;
2. The REFERENCE CASE is the fuel-only case at stoichiometric conditions;
3. In Figure 2 the turbulent intensity values at 700 CA deg. ATDC have been reported;
4. In Figure 3 the temperature difference reached at TDC with respect to fuel-only reference case at stoichiometric condition is visible for all cases of Table 5.

Table 5. PWI, DWI systems (best cases) and engine configurations - Operating points for reacting-flow analyses – Fixed rated power and Bmep target

CASE #	H2O INJ. SYST.	Parameter s [-]	Inj. Press [bar]	CR
W1		0.35	50.00	9.5
W2		0.35		9.5
W3	**DWI**	0.55	150.0	9.5
W4		0.35		10.5
W5	**PWI**	0.30	10.00	9.5
W6				10.5

Table 6. PWI and DWI systems – Injected fuel and water masses – Stoichiometric conditions

Case (λ 1.00)	Parameter s [-]	Fuel/Water injected mass [mg]
Fuel-only	-	84.00
Water-added	0.30	25.20
	0.35	29.40
	0.55	46.20

Table 7. Gasoline, Port Water and Direct Water injectors: injection timing

TYPE OF INJECTOR	Injection pressure [bar]	Parameter s [-]	SOI [CA deg. ATDCF]	EOI [CA deg. ATDCF]
GASOLINE	350.0	-	378	532
DWI	150.0	0.35	418	506
DWI	150.0	0.55	396	527
DWI	50.0	0.35	390	533
PWI	10.0	0.30	293	433

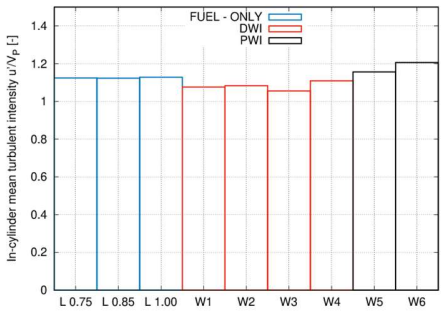

Figure 2. Turbulent intensity values at 700 CA deg. ATDC – Labels as in Table 5

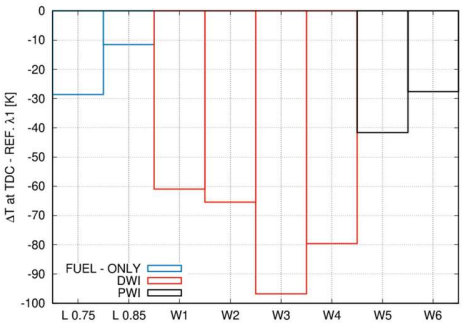

Figure 3. Temperature difference at TDC vs REFERENCE CASE λ 1.00 – Labels as in Table 5

5. In Figure 4 the mean mixture index distribution close to spark plug has been reported, in a volume enclosed in an ideal sphere of radius 10 mm and centered on the nominal spark plug location: in continuous line the DWI cases, in dashed line the PWI cases are visible. The target value has been 1.0. The mixture is a little lean for DWI cases, except in case of increased CR (W4 case). The mixture is richer that the target value for PWI cases.
6. Under the hypothesis of Gaussian distribution of the mixture index trend of Figure 4, in Figure 5 its standard deviation is visible. The standard deviation is not the same for PWI and DWI cases: it is lower for PWI cases than for DWI cases. The less the standard deviation, the less the cycle-by-cycle variation: the cycle-by-cycle repeatability increases moving from DWI to PWI architecture or, for DWI case, increasing the CR.

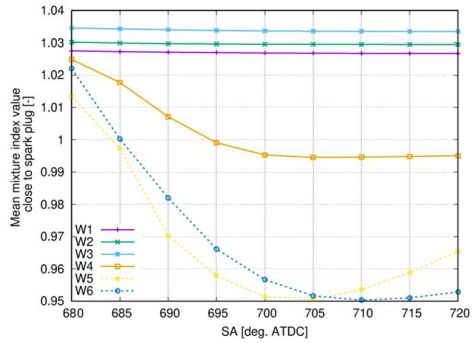

Figure 4. Mean mixture index close to spark plug at 700 CA deg. ATDC – R 10 mm – CASES WITH WATER ADDITION ONLY – Labels as in Table 5

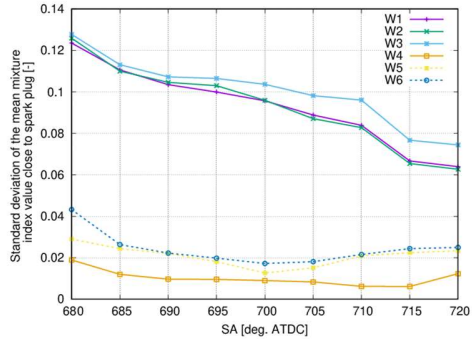

Figure 5. Standard deviation of the mean mixture index Gaussian distribution close to spark plug at 700 CA deg. ATDC – R 10 mm - CASES WITH WATER ADDITION ONLY – Labels as in Table 5

WATER INJECTION SYSTEM AND ENGINE CONFIGURATIONS: REACTING FLOW RESULTS

The engine map must be verified for the fulfillment of both engine knock-safe operations and exhaust gases TiT limit. As far as the latter is concerned, it must be considered that upcoming turbocharger technologies are increasing the TiT limits up to 1030-1050°C. Since the present work deals with 3D CFD in-cylinder simulations, the exhaust gas threshold temperature value representative of the TiT limit was taken as 1630 °C (that corresponds to 1903.15 K) at 800 CA deg. ATDCF, based on an estimation carried out in the OpenWAM 1D simulations.

In the present work, the incipient knock condition was identified by using as threshold MAPO limit the BOSCH criterion, which is obtained dividing the engine speed (in rpm) by 1000. A 4th order Butterworth band-pass filter between 5kHz and 20kHz for evaluating the MAPO has been applied to the pressure trace in a crank angle window between -10 and 80 crank angle degrees after top the dead center (ATDC) [30]. The pressure trace was

recorded by a virtual probe flush mounted on the cylinder head close to the location of the water injector (the probe location is the same for both configurations). Pursuing a practical approach in determining the Knock Limit Spark Advance (KLSA), the latter is identified by the Spark Advance (SA) undergoing the condition of incipient detonation minus 4 crank angle degrees to include the cycle to cycle variation stochastic effect. Moreover, it is to say that the combustion angles have been derived by the virtual transducer pressure trace using post-processing analysis methods as those used at the test bench for the indicating data analysis.

A brief overview on the combustion simulation WITHOUT water injection

The actual fuel enrichment strategy for limiting TiT below the threshold adopts a mixture index variable in the range among λ 0.75 and λ 0.85. The reference case for the present combustion strategy has been chosen to be λ 0.75: case λ 0.85 is a less favorable point for the combustion development, due to its higher temperature at TDC, as reported in [7]. The stoichiometric condition (λ 1.0) has been compared to both cases. Main results will be traced on the MFB50 (50% mass fraction burnt) parameter, which represents the combustion phasing of the engine [30].

The methodology here proposed, based on the detailed evaluation of the chemical properties of the mixture (and not only of the fuel), and therefore of its reactivity, allows properly simulating the evolution of the flame under variable quantities of water vapor, and not only as a function of pressure, temperature, mixture index, as well as EGR, whose chemical properties are different from those of the injected water, as already demonstrated [5, 6]. For the combustion analysis, in Figure 6 the trend of the MAPO value versus both the MFB50 and the mean exhaust temperature has been reported. In Figure 6b, where the MAPO versus the exhaust temperature is visible, only the SA laying in the bottom left of the graph, i.e. below the MAPO THRESHOLD and to the left of the EXHAUST TEMPERATURE THRESHOLD are truly workable. This area represents the 'acceptability zone': each SA falling outside this zone is not acceptable or because possible knock onset or because of exhaust gas temperature greater than the TiT or because of both. Depending on the mean mixture index, SA making the engine to work with MFB50 lower than 15-18 CA deg. are subject to detonation. The only feasible operating condition is that with λ 0.75 because it is the only one laying in the 'acceptability zone'. At full power condition, the engine might work only at λ 0.75. In fact, both the λ 1.0 and the λ 0.85 cases do not respect the maximum TiT temperature constraint at the knock limit advance points (below the YELLOW LINE of maximum MAPO). In Figure 7 the normalized IMEPH versus the MFB50 parameter is visible. The IMEPH value was computed in the range 640 – 800 CA deg. ATDCF. The reference IMEPH-TARGET value is that of the knock limit SA at λ 0.75 and it corresponds to the engine BMEP target. It must be noted that authors refer to IMEPH-TARGET rather than BMEP target to perform the comparison within the three-dimensional CFD simulation framework of analysis. The IMEPH value plotted in the picture was normalized by the IMPEH target value. A value of this ratio greater than 1.0 means an excessive load if compared to the target.

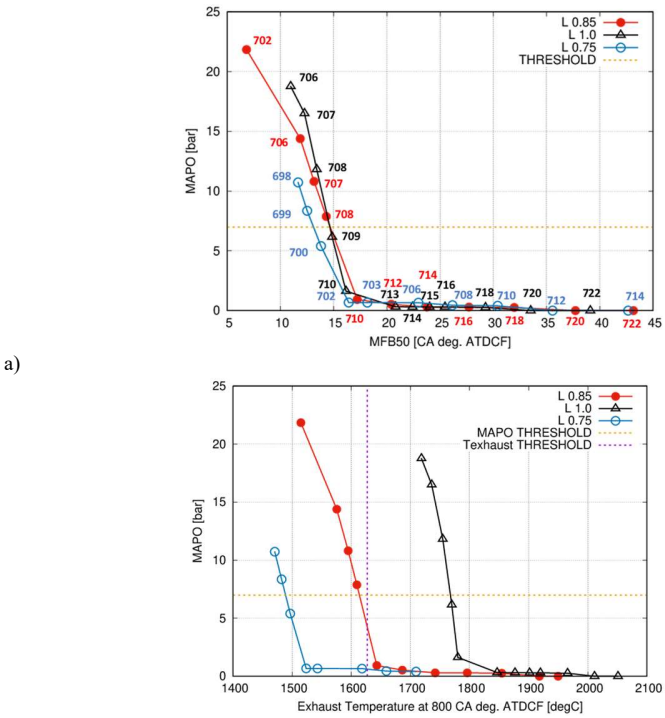

Figure 6. Maximum Amplitude of Pressure Oscillations versus: (a) MFB50; (b) Exhaust temperature at 800 CA deg. ATDC

In Figure 7 the knocking SA are in dashed lines. The knock limit SA for each mixture indexes considered is the one at the boundary between the dashed line and the continuous line. At fixed target IMEPH value, the KLSA at λ 0.75 is 703 CA deg. ATDCF, the KLSA at λ 0.85 is 712 CA deg. ATDCF and the KLSA at λ 1.00 is 713 CA deg. ATDCF. The in-cylinder thermal regime is higher for λ 0.85 and λ 1.00 than for λ 0.75 [5]. Case λ 0.85 reaches the same IMEPH of λ 1.00 but with a SA less of 1 degree. In order to understand this result, it is necessary to consider the evolution of the average flame front laminar flame speed in the case SA710 in Figure 8.

The average flame front laminar flame speeds of the cases λ 1.00 and λ 0.85 are quite the same except during the early combustion phase (which is indeed the most important phase of the premixed combustions), where the case λ 1.00 exhibits the faster laminar flame speed values because of the mixture inhomogeneity close to the spark plug at ignition time occurring in the case λ 0.85. The case λ 0.75 presents a much lower laminar flame speed because of the adopted air index. Thus, to achieve the target IMEPH the spark must be advanced of about 10 degrees, in order to compensate the slower flame laminar speed. This operation is made feasible without knock limitation due to the lowest in-cylinder thermal regime, as shown in Figure 3, where one can see that the case λ 0.75 provides the lowest unburnt gas temperature at TDC because of both the air index and the highest cooling.

For summarizing, the previous results show the limitation occurred in operating the engine at λ 0.85 and at λ 1.0 due to the higher thermal in-cylinder conditions than that occurring in the case at λ 0.75. The challenging is the fulfillment of the exhaust gas TiT limits. The temperature at 800 CA deg. ATDCF of the present engine should be lower than 1630 °C (1903,15 K), representative of the TiT limit for the turbine protection issues. Only the case at λ 0.75 fulfills the TiT limit. For both cases at λ 0.85 and at λ 1.00, this constraint is not satisfied since the TiT cannot be lowered by increasing the spark advance because of the knock onset.

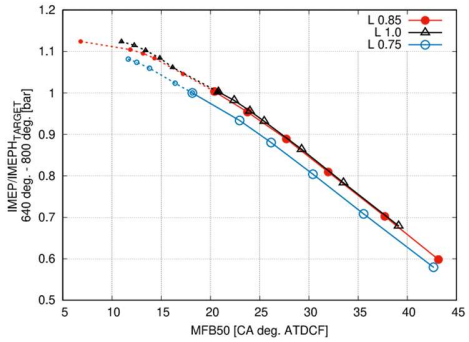

Figure 7. - IMEPH/IMEPTARGET swept versus MFB50 – KNOCKING SA in DASHED LINE

As a result, the stoichiometric case at full power, which may be likely required by new AES assessment policy, is expected to not largely fulfil the current (950 °C) turbocharging TiT limits and to hardly accomplish with the upcoming turbocharging TiT limits (1030°-1050°C). Thus, the challenge to deal with TiT limit running at stoichiometric condition is assessed in the next paragraph with the application of the water injection.

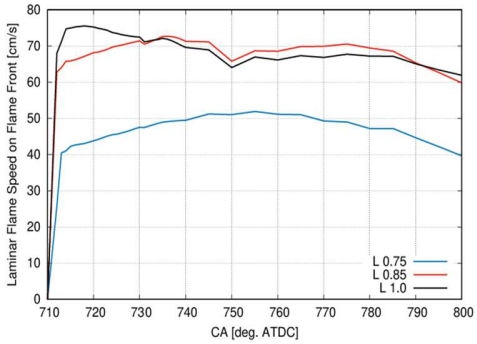

Figure 8. Laminar flame speed on flame front at SA710 CA deg. ATDCF.

Combustion simulation WITH water injection

Applying the water injection strategy, the fresh gases temperature has been reduced as a function of the injected water mass as shown in Figure 3 keeping in mind that all cases fulfill the constrain of achieving at least the 90% of injected water evaporation. Therefore, it is possible to start drawing some considerations about the key points of the forthcoming combustion analysis:

1. The two results expected by using the water injection is to accomplish with TiT limits and then to achieve a more advanced combustion phasing thanks to the expected weaker knocking attitude.
2. On the other hand, it is necessary to keep in mind that the water acts as inert gas penalizing:
    a. The polytropic index of the mixture, which limits the indicated efficiency enhancement.
    b. The laminar flame speed of the burning mixture by its presence in the vapor state.
    c. Again, the laminar flame speed due to the lower fresh mixture temperature because of the water cooling effect.
3. From the above statements, it is clear that there is an '*a priori*' penalization of the combustion provided by the water injection concept, with the risk of not achieving any gain on TiT reduction. In this contest, approaches based on the detailed chemistry are mandatory to perform accurate assessments of the water injection system technology and related engine operations.

The best configurations tested for PWI and DWI solutions have been summarized in Table 5: they will be analyzed in detail considering in first step the cases with the same engine compression ratio (i.e., CR=9.5).

Engine type: CR 9.5 – PWI vs DWI

In Figures 9 and 10 are shown the normalized IMEPH curves versus MFB50, the MAPO traces versus MFB50 and exhaust temperature at 800 CA deg. ATDCF, respectively. It is clearly visible that the DWI strategy never shows knock onset at the injection pressure of 150 bar because the MAPO curves never approach the threshold line of 7 bar, while it detonates at 50 bar for SA694 (Figure 10). At this KLSA angle the MFB50 crank angle occurs at 6.0 CA deg. ATDCF. The amount of injected water vaporized has increased the tolerability threshold of the engine to a faster cycle than the average one typical of this type of engine. In Figure 10b it is to note that the case *s 0.35* 50 bar cannot reach the 'acceptability area', i.e. it is not possible to lower the temperature below the threshold temperature and, at the same time, to keep the MAPO in the safe zone. Looking at Figure 9, the DWI solution allows to advance the SA resulting in higher IMEPH values which are above the target one. The spark advancement allows speeding up the combustion and it reduces the exhaust temperature too. Therefore, a high IMEPH is obtained with the same FUEL CONSUMPTION, that means a reduction of the *bsfc*. In general, it can be stated that DWI systems provide lower in-cylinder thermal load (lower fresh gases temperature at TDC) than that provided by PWI resulting in a *bsfc* gain. Nevertheless, it must be pointed out that the in-cylinder exhaust gases temperature at 800 ca deg. ATDCF does not fall below the threshold because of the slowdown of the flame speed. The last is linked both to the presence of significant mass fractions of water in the vapor state and to the drop of the mixture temperature. The laminar flame speed is mainly influenced by these last two parameters, mostly the quantity of vaporized water.

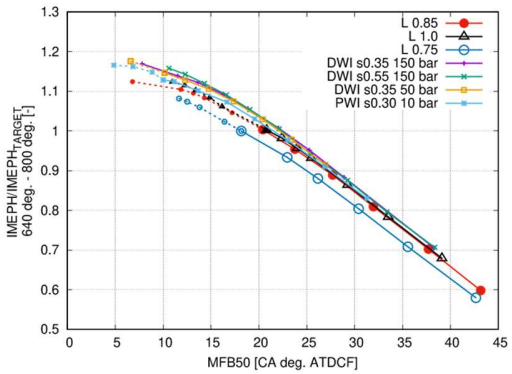

Figure 9. - IMEPH/IMEPTARGET swept vs MFB50 – KNOCKING SA in DASHED LINE

In Figure 11 the combustion durations MFB10-MFB50 and MFB50-MFB90 are shown. Keeping constant the *s* parameter at *0.35*, it is to note that the low pressure DWI case (p 50 bar) provides the same combustion phase as the high pressure DWI (p 150 bar) strategy, but it provides little higher fresh mixture temperatures than those achieved by the high pressure DWI case (150 bar), as visible in Figure 12 where the unburnt temperature profile has been plotted at SA706. In Figure 11 for both combustion durations one can see very clearly that the case with s 0.55 provides too slow combustion duration and it does not reach the 99% of MFB neither using at SA 702 CA deg. ATDC because of both the amount of evaporated water mass dilution effect and the much low fresh gases temperatures. As an overall result, a slowdown of the combustion process occurs. Therefore, the case s 0.55 is not practically feasible because of the too long combustion duration.

Summarizing what has been stated so far:

1. The laminar flame speed is MAINLY INFLUENCED by the reactivity of the mixture, therefore by the chemical properties the mixture assumes depending on the quantity of vaporized water, which lowers the temperature but also acts as an inert. Accurate modeling of the chemistry is thus mandatory in order to properly assess the combined effects of the water injection.
2. The DWI case s 0.55 at p 150 bar leads to a much lower fresh gases temperature at TDC at the expense of an excessive combustion slowdown. Therefore, from the current results it is not of interest for engine applications.

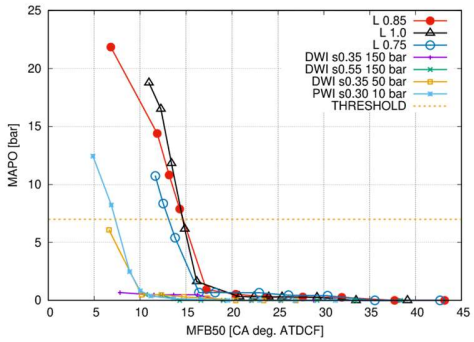

(a)

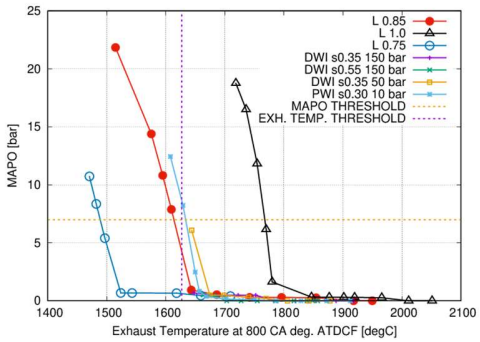

(b)

Figure 10. Maximum Amplitude of Pressure Oscillations versus: (a) MFB50; (b) Exhaust temperature at 800 CA deg. ATDC

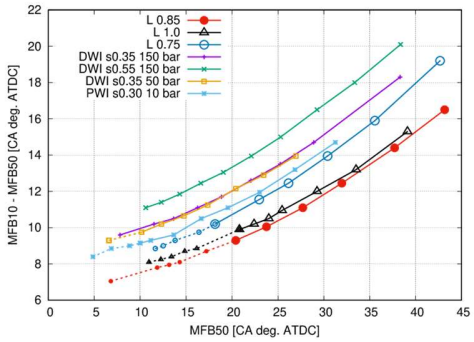

(a)

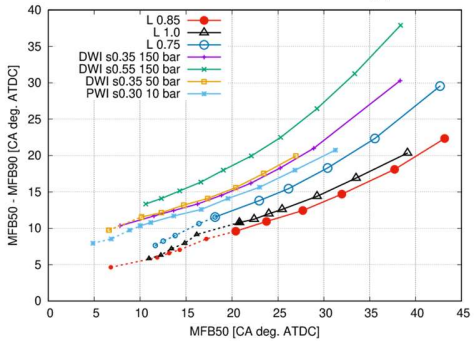

(b)

Figure 11. – Combustion duration vs MFB50: (a) MFB10 to MFB50; (b) MFB50 to MFB90

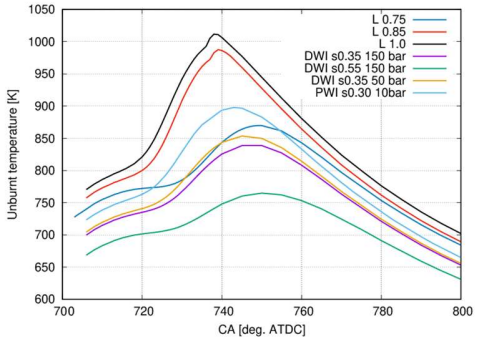

Figure 12. Mean temperature of the unburnt mixture at SA706 CA deg. ATDCF.

The above presented results for DWI strategy show that the achievable load is greater than expected (BMEP TARGET 26.6 bar), so it is certainly possible to reduce the quantity of fuel, which in itself already reduces the engine exhaust temperature and in general the thermal load of the engine

cycle. The cooling margin in comparison with the rich mixture solution (λ 0.75) allows investigating solutions with increased CR, which is limited in the present work to CR 10.5 for engine geometry reasons.

Engine type: CR 10.5 – PWI vs DWI

In this paragraph the cases at CR 10.5, DWI s 0.35 - 150 bar and PWI s 0.30 - 10 bar are analyzed, respectively. The simulations have been performed keeping constant the trapped air mass and thus the fuel mass, under stoichiometric conditions. The CR increase brings a thermodynamic efficiency increase, which induces an effective increase of the output power. The latter is visible in the IMEPH increase during the combustion process. Thus, for having the same rated power of the baseline engine, it would be necessary to reduce both the fuel consumption and the trapped mass, reducing the boost pressure of the turbocharger.

Figures 13 and 14 depict the normalized IMEPH curve versus MFB50, the MAPO curves versus MFB50 and exhaust temperature at 800 CA deg. ATDCF, respectively. In Figure 15 the laminar flame speed on the flame front is presented for both DWI and DWI solutions. By them it is possible to compare DWI and PWI systems:

1. For the same target IMEPH value, the DWI system gains 1 deg. in the SA at the same exhaust temperature.
2. Looking at the KLSA, so considering the maximum performances of the engine, the DWI system gains 6 CA deg. in the knock limit SA, resulting in a 1% increment of the IMEPH value and the exhaust temperature reduces of almost 100.0 K.
3. The CR increase induces higher an average flame front laminar flame speed (Figure 15). The laminar flame speed results higher for PWI strategy than for DWI strategy because of both the higher thermal regime associated to the PWI solution and the lower amount of injected water vapor mass (s 0.30 instead of s 0.35).

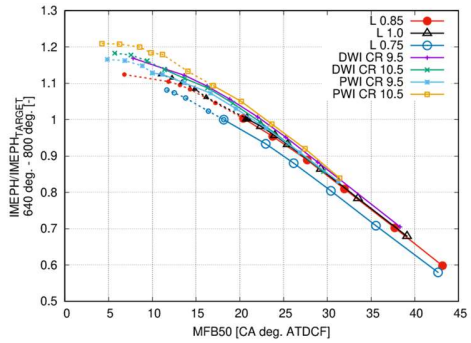

Figure 13. - IMEPH/IMEPTARGET swept vs MFB50 – KNOCKING SA in DASHED LINE – DWI: s 0.35 150 bar – PWI: s 0.30 10 bar

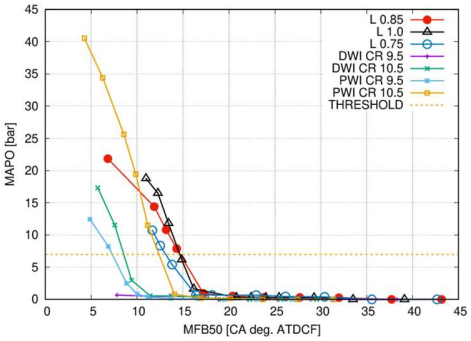

(a)

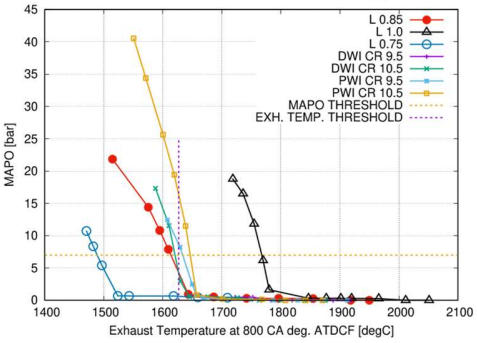

(b)

Figure 14. Maximum Amplitude of Pressure Oscillations versus: (a) MFB50; (b) Exhaust temperature at 800 CA deg. ATDC – DWI: s 0.35 150 bar – PWI: s 0.30 10 bar

It is also possible to compare the effect of the increased CR for the same water injection system:

DWI: Increasing the CR of 1.0 point in the DWI system, the knock limit SA is retarded of 2 crank angle degrees, while the IMEPH remains almost the same. The exhaust temperature is reduced of 40.0 K. At SA 700 CA deg. ATDCF, which is the knock limit SA for DWI CR 10.5, the exhaust temperature reduction reduces of about 77.0 K if compared to the same system having CR 9.5. The last is due to the more efficient combustion process linked to the increased thermodynamic efficiency, which reduces the combustion angles. In general, the increase of the compression ratio of 1.0 point leads to an increment of the IMEPH (Figure 13). The IMEPH value, at the same SA, increases of about 2%. It is possible to reduce the fuel consumption, as just observed before. Increasing the injected water mass, at the same SA the IMEPH gets reduced because of the slowdown of the combustion (MFB50 lengthening). The DWI solution at increased CR reaches the knock onset because the combustion duration is a little higher (Figure 16) but the fresh mixture temperature is higher too.

PWI: Increasing the CR of 1.0 point in the PWI system, the knock limit SA is advanced of 5 degrees, i.e. it is 706.0 CA deg. ATDCF instead of 701.0 CA deg. ATDCF. The exhaust temperature increases from 1925.0 K to 1974.3 K.

Summarizing, in PWI system the CR increase induces an advance of the knock limit SA with a loss of 35.0 K in the exhaust temperature, and the IMEPH target is reached at SA 709.0 CA deg. ATDCF instead of 710.0 CA deg. ATDCF, with a reduction in the exhaust temperature of 30.0 K. Globally there is a not appreciable lengthening of the combustion duration increasing the CR in PWI systems (Figure 16).

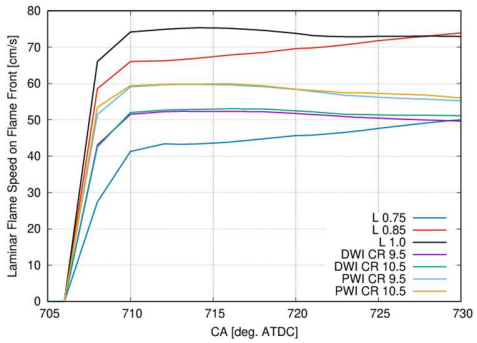

Figure 15. Laminar flame speed on flame front at SA706 CA deg. ATDCF.

The increase of CR reduces the cooling effect of the water in the compression stroke (at the same IMEPH, it is not worth mentioning) but it is found to: a) increase the thermodynamic efficiency thanks to the longer expansion phase and to the flame front higher laminar flame speeds (Figure 15) which shortens the combustion durations; b) reduce the exhaust gas TiT value, as overall results of the previous point.

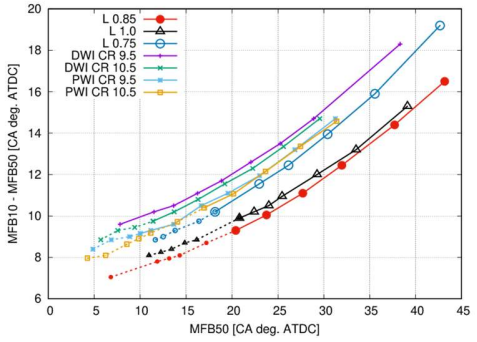

(a)

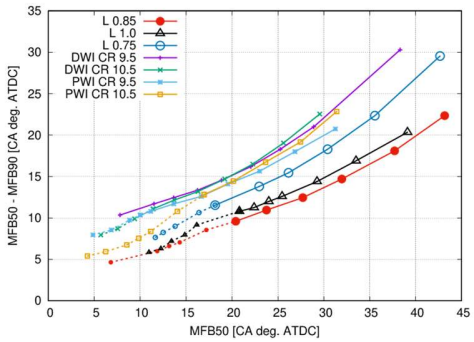

(b)

Figure 16. – Combustion duration vs MFB50: (a) MFB10 to MFB50; (b) MFB50 to MFB90 – DWI: s 0.35 150 bar – PWI: s 0.30 10 bar

Final comparison

In this paragraph a brief comparison has been reported. In Figure 17 the Knock Limit SA (KLSA) for all cases of Table 5 plus fuel-only cases have been traced. The reference case is λ 0.75, with KLSA at 703 CA deg. ATDC: it provides an IMEPH equal to the target one (Figure18) and an exhaust temperature below the threshold value of 1630 °C (Figure 19). In Figure 20 the MFB50 angles corresponding, for each case, to the KLSA of Figure 17 are visible.

The above reported combustion results have shown that the same IMPEH target is reached for a reduced SA with respect to the solution without water, but the exhaust temperature does not still satisfy the constraint of the TiT limit. Once again, this is due to the combined effect of the lower fresh gases temperatures and the dilution effects correlated to the water addition. The water injection slows down the combustion process and thereby the spark timing needs to be advanced for obtaining the target IMEPH. For reducing the exhaust temperature, it is necessary to advance further the SA, with a reduction the fuel consumption for the considered operating point in order to maintain the engine load IMPH target. but with a reduced quantity of fuel.

Looking at these last reported pictures, it might be highlighted that:

1. Fuel-only cases: λ 0.85 and λ 1.00 have a more retarded KLSA than λ 0.75 (Figure 17) with about the same IMEPH (Figure 18). This is due to a lengthening of the combustion process, visible in a greater MFB50 angle (Figure 20) and resulting in an increased exhaust temperature at 800 CA deg. ATDC, as shown in Figure 19.

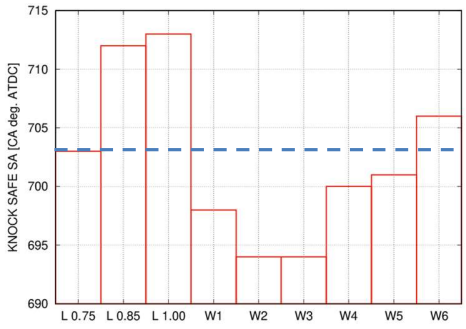

Figure 17. KLSA values for all cases of Table 5 – COMPARISON – BLUE LINE is the REFERENCE value at λ 0.75

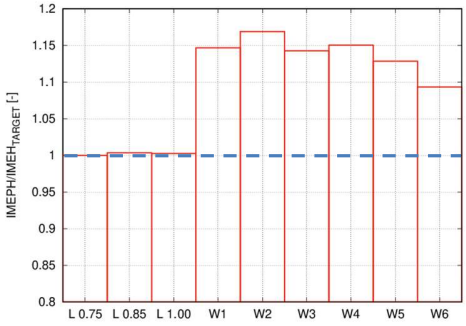

Figure 18. IMEPH/IMEPTARGET at KLSA for all cases of Table 5 - COMPARISON – BLUE LINE is the REFERENCE value at λ 0.75

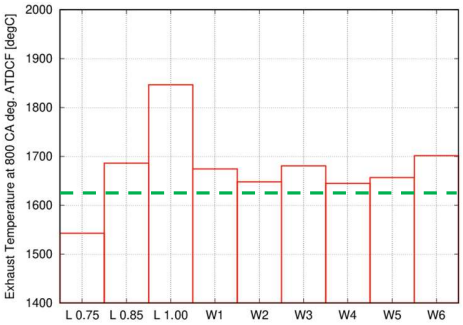

Figure 19. Exhaust temperature at 800 CA deg. ATDCF at KLSA for all cases of Table 5 – COMPARISON – GREEN LINE is the TiT TRESHOLD VALUE

2. DWI at both CR values (from W1 to W4) and PWI at CR 9.5 (W5) have a KLSA more advanced that λ 0.75 case with an increased IMEPH with respect to the target one, except for PWI case at CR 10.5. It would be possible to reduce the load, thus the *bsfc*, for having the same engine load. This load increase is related to an overall best efficiency. The MFB50 angle is less than at λ 0.75. The exhaust temperature is above the TiT threshold imposed but it could be lowered together with the *bsfc* reduction.

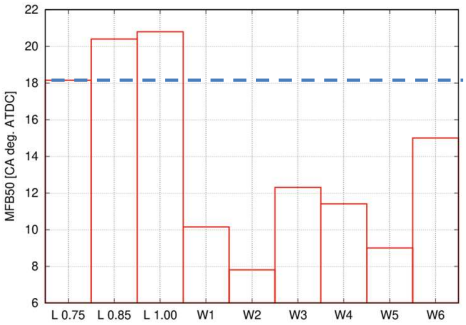

Figure 20. MFB50 degrees at KLSA for all cases of Table 5 - COMPARISON – BLUE LINE is the REFERENCE value at λ 0.75

Conclusions

Adding water makes the knock analysis more complex than ever because the main role is played by the mixture reactivity rather than the fuel. Therefore, the accurate evaluation of the chemical properties of the mixture is crucial for addressing the engine designers towards the best solution.

At industrial and research level, significant efforts are currently being made to equip the cars with electric compressors, which would eliminate the turbine and so the problem of the exhaust temperature limit. On the other hand, in the last scenario, high exhaust gases temperature means WASTED ENERGY that cannot be afforded at all. So, this research has value regardless of whether the turbine is present in the near future or not. In any case the research must be oriented towards an increase of the thermodynamic efficiency of the engine, therefore towards both reduced wall losses and less fuel consumption in the engine. Moreover, all the water injection solution investigated were selected among those provided an injected water vaporization above 90 %.

Summarizing the main combustion results:

1. Cases λ 1.0 and λ 0.85 have rapid combustion thanks to the higher thermal regime without water dilution and to favorable equivalence ratio, but the thermal regime leads them to detonation or in any case to excessive exhaust temperature if compared to the TiT threshold.
2. PWI cases result in higher laminar flame speed than those provided by DWI solutions because the water quantity is lower, i.e. s 0.30 vs s 0.35.
3. For DWI s 0.35 p 150 bar case IMEPH lies between λ 1.0 - λ 0.85 cases and λ 0.75. This configuration does not detonate because the fresh gas temperature regime remains low case.
4. DWI s 0.35 p 150 bar case results in the strongest fresh gases cooling which is counterbalanced by a heavy slowdown of the combustion process.
5. By considering a compression ratio CR 9.5, only with λ 0.75 strategy and DWI system s 0.35 150 bar it is possible to reach an exhaust temperature values below the threshold. In case of DWI it is necessary to advance consistently the ignition timing with respect to the case λ 0.75 to counterbalance the longer combustion duration.
6. For the same DWI case (s 0.35) with CR 10.5, apparently it is not possible to drop the temperature below the threshold because of the limited evaporation rate which affects strongly the cooling effect, but it is necessary to keep in mind that these performances are reached

with a higher load. Reducing the load, it is admissible to think that this temperature threshold can be reached, also considering the new TiT limits allowed by the upcoming turbocharger technology advancements.

7. DWI system performances are always better than those of the PWI system, which represents the least expensive solution and then the research on it should be continued in authors' opinion with addition of other technologies like overexpanded cycle or variable compression ratio, to cite a few.

References

1. Cordier, M., Lecompte, M., Malbec, L.-M., Reveille, B. et al., "Water Injection to Improve Direct Injection Spark Ignition Engine Efficiency," SAE Technical Paper 2019-01-1139, 2019, doi:10.4271/2019-01-1139.
2. Pulga, L., Falfari, S., Bianchi, G.M., Ricci, M. et al., "Advanced Combustion Modelling of High BMEP Engines under Water Injection Conditions with Chemical Correlations Generated with Detailed Kinetics and Machine Learning Algorithms," SAE Technical Paper 2020-01-2008, 2020, doi:10.4271/2020-01-2008
3. Stefania Falfari, Gian Marco Bianchi, Giulio Cazzoli, Claudio Forte, Sergio Negro, "Basics on Water Injection Process for Gasoline Engines", Energy Procedia (2018) pp. 50-57 DOI information: 10.1016/j.egypro.2018.08.018.
4. Falfari, S., Bianchi, G.M., Cazzoli, G., Ricci, M. et al., "Water Injection Applicability to Gasoline Engines: Thermodynamic Analysis," SAE Technical Paper 2019-01-0266, 2019, doi:10.4271/2019-01-0266.
5. Giulio Cazzoli, Gian Marco Bianchi, Stefania Falfari, Claudio Forte, "Development of a chemical-kinetic database for the laminar flame speed under GDI and water injection engine conditions", Energy Procedia (2018) pp. 154-161 DOI information: 10.1016/j.egypro.2018.08.043.
6. Cazzoli, G., Bianchi, G.M., Falfari, S., Ricci, M. et al., "Evaluation of Water and EGR Effects on Combustion Characteristics of GDI Engines Using a Chemical Kinetics Approach," SAE Technical Paper 2019-24-0019, 2019, doi:10.4271/2019-24-0019.
7. S. Falfari, G. Cazzoli, M. Ricci, C. Forte, " PWI and DWI Systems in Modern GDI Engines: Optimization and Comparison - Part I: Non-Reacting Flow Analysis", *submitted to WCX 2021, SAE Congress, Detroit: Michigan, USA.*
8. Rohit, A., Satpathy, S., Choi, J., Hoard, J. et al., "Literature Survey of Water Injection Benefits on Boosted Spark Ignited Engines," SAE Technical Paper 2017-01-0658, 2017, doi:10.4271/2017-01-0658.
9. Gerty, M. and Heywood, J., "An Investigation of Gasoline Engine Knock Limited Performance and the Effects of Hydrogen Enhancement," SAE Technical Paper 2006-01-0228, 2006, doi:10.4271/2006-01-0228.
10. Poinsot, T., Veynante, D., "Theoretical and Numerical Combustion", 2001, Edwards, 9781930217058
11. Dekena, M., Peters, N., "Combustion modeling with the G-equation", Oil Gas Sci. Technol. 54 (1999) 265–270
12. Colin O., Benkenida A. "The 3-Zone Extended Coherent Flame Model (ECFM3Z) for computing premixed/diffusion combustion", Oil Gas Sci. Technol. -Rev. IFP 59, 6, 593-609.
13. Metghalchi, M., Keck, J., 1982. "Burning velocities of mixtures of air with methanol, isooctane, and indolene at high pressure and temperature". Combustion and Flame, 48(C), pp. 191-210.
14. Cazzoli, G., Forte, C., Bianchi, G., Falfari, S., Negro, S., "A Chemical-Kinetic Approach to the Definition of the Laminar Flame Speed for the Simulation of the Combustion of Spark-Ignition Engines", SAE Technical Paper 2017-24-0035, 2017, DOI: 10.4271/2017-24-0035.
15. Fandakov, A., Grill, M., Bargende, M., and Kulzer, A.C., "A Two-Stage Knock Model for the Development of Future SI Engine Concepts," SAE Technical Paper 2018-01-0855, 2018, doi:10.4271/2018-01-0855.
16. Fandakov, A., Grill, M., Bargende, M., and Kulzer, A., "Two-Stage Ignition Occurrence in the End Gas and Modeling Its Influence on Engine Knock," SAE Int. J. Engines 10(4):2017, doi:10.4271/2017-24-0001.
17. Pulga, L., Bianchi, G.M., Falfari, S. e Forte, C." A Machine Learning Methodology For Improving the Accuracy of Laminar Flame Simulations with Reduced Chemical Kinetics Mechanisms", Combustion and Flame, Vol. 216, pp 72-81, https://doi.org/10.1016/j.combustflame.2020.02.021, 2020.
18. Pulga, L., Bianchi, G., Ricci, M., Cazzoli, G. et al., "Development of a Novel Machine Learning Methodology for the Generation of a Gasoline Surrogate Laminar Flame Speed Database under Water Injection Engine Conditions," SAE Int. J. Fuels Lubr. 13(1):5-17, 2020, https://doi.org/10.4271/04-13-01-0001.
19. F. Berni, S. Breda, M. Lugli, G. Cantore, "A numerical investigation on the potentials of water injection to increase knock resistance and reduce fuel consumption in highly downsized GDI engines", Energy Procedia (2015), pp. 826-835, doi: 10.1016/j.egypro.2015.12.091.
20. Battistoni, M., Grimaldi, C., Cruccolini, V., Discepoli, G. et al., "Assessment of Port Water Injection Strategies to Control Knock in a GDI Engine through Multi-Cycle CFD Simulations," SAE Technical Paper 2017-24-0034, 2017, doi:10.4271/2017-24-0034.
21. Netzer, C., Franken, T., Seidel, L., Lehtiniemi, H. et al., "Numerical Analysis of the Impact of Water Injection on Combustion and Thermodynamics in a Gasoline Engine Using Detailed Chemistry," SAE Technical Paper 2018-01-0200, 2018, doi:10.4271/2018-01-0200.
22. De Bellis, V., Bozza, F., Teodosio, L., and Valentino, G., "Experimental and Numerical Study of the Water Injection to Improve the Fuel Economy of a Small Size Turbocharged SI Engine," SAE Int. J. Engines 10(2):550-561, 2017, https://doi.org/10.4271/2017-01-0540.
23. Iacobacci, A., Marchitto, L., and Valentino, G., "Water Injection to Enhance Performance and Emissions of a Turbocharged Gasoline Engine under High Load Condition," SAE Int. J. Engines 10(3):928-937, 2017, https://doi.org/10.4271/2017-01-0660.
24. Raut, A. and Mallikarjuna, J., "Effects of Water Injector Spray Angle and Injector Orientation on Emission and Performance of a GDI Engine—A CFD Analysis," SAE Int. J. Engines 13(1):17-33, 2020, doi:10.4271/03-13-01-0002.
25. Gern, M. S., Vacca, A., and Bargende, M., "Experimental Analysis of the Influence of Water Injection Strategies on DISI Engine Particle Emissions," SAE Technical Paper 2019-24-0101, 2019, doi:10.4271/2019-24-0101.
26. Vacca, A., Bargende, M., Chiodi, M., Franken, T. et al., "Analysis of Water Injection Strategies to Exploit the Thermodynamic Effects of Water in Gasoline Engines by Means of a 3D-CFD Virtual Test Bench," SAE Technical Paper 2019-24-0102, 2019, doi:10.4271/2019-24-0102.
27. Millo, F., Mirzaeian, M., and Porcu, D., "Knock Mitigation Techniques for Highly Boosted Downsized SI Engines," SIA Powertrain, 2017.

28. Paltrinieri, S., Mortellaro, F., Silvestri, N., Rolando, L. et al., “Water Injection Contribution to Enabling Stoichiometric Air-to-Fuel Ratio Operation at Rated Power Conditions of a High-Performance DISI Single Cylinder Engine,” SAE Technical Paper 2019-24-0173, 2019, doi:10.4271/2019-24-0173.
29. Brusiani, F., Bianchi, G., and Tiberi, A., “Primary Breakup Model for Turbulent Liquid Jet Based on Ligament Evolution,” SAE Technical Paper 2012-01-0460, 2012, https://doi.org/10.4271/2012-01-0460
30. Forte, C., Corti, E., Bianchi, G., Falfari, S. et al., "A RANS CFD 3D Methodology for the Evaluation of the Effects of Cycle By Cycle Variation on Knock Tendency of a High Performance Spark Ignition Engine", SAE Technical Paper 2014-01-1223, 2014, doi:10.4271/2014-01-1223.

Contact Information

For further information/details please contact:

Dr. Stefania Falfari: stefania.falfari@unibo.it

Prof. Gian Marco Bianchi: gianmarco.bianchi@unibo.it